

Identification of dysregulated genes and pathways of different brain regions in Alzheimer's disease

Yaping Wang & Zhiyun Wang

To cite this article: Yaping Wang & Zhiyun Wang (2020): Identification of dysregulated genes and pathways of different brain regions in Alzheimer's disease, International Journal of Neuroscience, DOI: [10.1080/00207454.2020.1720677](https://doi.org/10.1080/00207454.2020.1720677)

To link to this article: <https://doi.org/10.1080/00207454.2020.1720677>



Published online: 05 Feb 2020.



Submit your article to this journal 



View related articles 



View Crossmark data 

ORIGINAL ARTICLE



Identification of dysregulated genes and pathways of different brain regions in Alzheimer's disease

Yaping Wang and Zhiyun Wang

Department of Neurology, Tianjin First Central Hospital, Nankai District, Tianjin, China

ABSTRACT

Background: Alzheimer's disease (AD) is a degenerative neurologic disease. The study aimed to identify the key differentially expressed genes (DEGs) and pathways in AD pathogenesis and obtain potential biomarkers in AD diagnosis.

Methods: An integrated analysis of publicly available Gene Expression Omnibus datasets of AD was performed. DEGs in hippocampus tissue (HIP), temporal gyrus tissue (TG), frontal gyrus tissue (FG) and whole blood (WB) were identified. Bioinformatics analyses were used to insight into the functions of DEGs. The expression levels of candidate DEGs were preliminarily validated in GSE1297. The discriminatory ability of candidate DEGs in WB samples of AD patients and healthy individuals was evaluated in GSE63060 and GSE63061 datasets through receiver operating characteristic (ROC) analysis.

Results: The DEGs in HIP, TG and FG tissues of AD were identified. Functions involved in regulation of apoptotic process, apoptotic process and cell death were significantly enriched from DEGs in AD. MAPK signaling pathway and Wnt signaling pathway were significantly enriched. YAP1, MAPK9 and GJA1 were the hub proteins in protein–protein interaction network in HIP, TG and FG. The expression levels of 14 DEGs in GSE1297 dataset were consistent with our integrated analysis. Moreover, 7 out of 14 DEGs had the diagnostic value in distinguishing AD patients from healthy controls in both GSE630060 and GSE630061 datasets.

Conclusion: The DEGs including YAP1, MAPK1, GJA1 and pathways including MAPK signaling pathway and Wnt signaling pathway may be related to AD progression. RAD51C, SAFB2, SSH3 and TXNDC9 might be potential biomarkers in AD diagnosis.

ARTICLE HISTORY

Received 1 June 2019

Revised 14 November 2019

Accepted 14 January 2020

KEYWORDS

Alzheimer's disease;
pathogenesis; diagnosis

Introduction

Alzheimer disease (AD) is a chronic and progressive neurodegenerative disease. It is characterized by brain atrophy, progressive memory loss and cognitive impairment. Brain pathological hallmarks of AD include neuronal loss, accumulation of amyloid β (A β) plaques in the brain parenchyma and neurofibrillary tangles in the neurons [1,2].

The occurrence and development of AD is affected by age, genetic variants, traumatic brain injury, cardiovascular disease, environmental factors, circadian disruption and other factors. The neuronal dysfunction and cell death mechanisms are commonly found in AD, which are caused by production of high levels of cytokines and the formation of amyloid plaques. It is reported that a series of dysregulated genes are involved in AD progression. Dysregulation of Cdk5 contributes to pathological events in AD including

formation of senile plaques and neurofibrillary tangles, synaptic damage, mitochondrial dysfunction and neuronal cell apoptosis [3,4]. Aberrant RCAN1 expression contributes to neuronal apoptosis and Tau hyperphosphorylation, resulting in neuronal loss and neurofibrillary tangle formation [5]. TREM2 is involved in AD neuropathology including amyloid- β deposition, tau hyperphosphorylation, neuroinflammation and neuronal and synaptic losses in AD animal model [6–8]. Autophagic dysfunction plays a fundamental role in the formation and propagation of AD. Increasing research suggested that autophagy shows a central role in the metabolism of A β , and it encourages the secretion of A β and remarkably contributes to Alzheimer's pathology [9]. Melatonin, a pineal gland-synthesized neurohormone, plays neuroprotective roles in inhibition of circadian disruption by controlling clock genes, attenuating A β accumulation and tau hyperphosphorylation by regulating

glycogen synthase kinase-3 (GSK3) and cyclin-dependent kinase-5 (CDK5) signaling pathway [10]. Genistein (4',5,7-trihydroxyisoflavone), a soy-derived isoflavone and phytoestrogen, suppresses Alzheimer's pathology by regulating copious intracellular events, such as reducing the formation of neurotoxic A β by activation of PKC signaling, decreasing A β generation by downregulation of the transmembrane protein presenilin, reduction of oxidative stress, suppression of mitochondrial damage, inhibition of cell apoptosis, downregulation of the neuroinflammatory signaling, improvement of the spatial memory and learning [11]. Despite the fact that remarkable advances have been made in the understanding of AD, the pathophysiology mechanism of AD is not well understood.

In this study, we performed an integrative analysis of available Gene expression profiling of brain tissues includes hippocampus tissue (HIP), temporal gyrus tissue (TG), frontal gyrus tissue (FG) and whole blood (WB) from AD patients and normal controls. Our work aimed to identify the key differentially expressed genes (DEGs) and pathways in AD pathogenesis and obtain potential biomarkers in AD diagnosis, which might provide valuable information for the identification of diagnostic biomarkers and therapeutic targets for AD in future study.

Materials and methods

Ethics

Our work was approved by the ethics committee of Tianjin First Central Hospital.

Gene expression datasets

The GEO database (www.ncbi.nlm.nih.gov/geo/) is an international public repository that distributes high-throughput gene expression datasets [12]. In order to explore the differences of expression profiling and relevant biological processes in AD patients, we searched datasets from the GEO database with the keywords 'alzheimer disease'[MeSH Terms] OR Alzheimer's disease[All Fields] AND 'Homo sapiens'[-porgn] AND 'gse'[Filter].The inclusion and exclusion criteria were as follows: datasets should be the whole-genome expression data; whole-genome expression data should be obtained from HIP, TG, FG and WB samples of AD patients and normal controls. Finally, six microarray datasets generated from HIP [13–18] (five datasets including GSE48350, GSE29378, GSE36980, GSE28146 and GSE5281 were used to identify DEGs and one dataset GSE1297 was used to validate DEGs), three datasets generated from FG [13,15,17]

(including GSE48350, GSE36980 and GSE5281), three datasets generated from TG [15,17,19] (including GSE36980, GSE37263 and GSE5281) and four datasets generated from WB samples [20,21] (including GSE97760, GSE63060, GSE63061 and GSE18309) of AD patients and corresponding controls were incorporated into our studies. The detail information of datasets is shown in Table 1.

Identification of differentially expressed genes

Different microarray platforms are known to commonly cause heterogeneity among different microarray datasets, which makes it difficult to compare microarray dataset directly. In order to minimize the heterogeneity among different datasets in our study, normalization and log₂ transformation were performed for the raw data. Then, an R package metaMA was used to combine data from multiple microarray datasets [22]. Individual *p* values were calculated, and multiple comparison correction false discovery rate (FDR) was obtained by using the Benjamini & Hochberg method. Genes with FDR < 0.01 were screened out and regarded as DEGs. In our work, the DEGs in HIP, TG, FG and WB of AD patients compared with corresponding healthy individuals were respectively identified.

Functional enrichment

The underlying functions of DEGs in AD were predicted by the Gene Ontology (GO) function and Kyoto Encyclopedia of Genes and Genomes (KEGG) pathway enrichment analysis through online software Genecodis3 (<http://genecodis.cnb.csic.es>) [23]. FDR < 0.05 was set as the cutoff for selecting significant GO terms and KEGG pathway.

Network construction of protein–protein interaction

The complex cellular functions are undertaken by tightly interaction among proteins. BioGRID, a database of known and predicted protein interactions, was used to identify interacting protein pairs [24]. PPI network among DEGs was constructed by Cytoscape (<http://cytoscape.org/>) [25].

Validated the expression levels of DEGs in GSE1297 dataset

In order to analyze whether common DEGs were dysregulated in AD, the expression level of representative DEGs was preliminarily validated in GSE1297 dataset,

Table 1. The detail information of datasets.

Dataset ID	Cases of HC	Cases of AD	Platform	Country/Region	Author
HIP (6 datasets, 115 HC vs 111 AD)					
GSE48350	43	19	GPL570 [HG-U133_Plus_2] Affymetrix Human Genome U133 Plus 2.0 Array	USA	Nicole Claudia Berchtold
GSE29378	32	31	GPL6947 Illumina HumanHT-12 V3.0 expression beadchip	USA	Jeremy Miller
GSE36980	10	7	GPL6244 [HuGene-1_0-st] Affymetrix Human Gene 1.0 ST Array [transcript (gene) version]	Japan	Yusaku Nakabeppu
GSE28146	8	22	GPL570 [HG-U133_Plus_2] Affymetrix Human Genome U133 Plus 2.0 Array	USA	Eric M Blalock
GSE5281	13	10	GPL570 [HG-U133_Plus_2] Affymetrix Human Genome U133 Plus 2.0 Array	USA	Winnie Liang
GSE1297	9	22	GPL96 [HG-U133A] Affymetrix Human Genome U133A Array	USA	Eric M Blalock
FG (3 datasets, 77 HC vs 59 AD)					
GSE48350	48	21	GPL570 [HG-U133_Plus_2] Affymetrix Human Genome U133 Plus 2.0 Array	USA	Nicole Claudia Berchtold
GSE36980	18	15	GPL6244 [HuGene-1_0-st] Affymetrix Human Gene 1.0 ST Array [transcript (gene) version]	Japan	Yusaku Nakabeppu
GSE5281	11	23	GPL570 [HG-U133_Plus_2] Affymetrix Human Genome U133 Plus 2.0 Array	USA	Winnie Liang
TG (3 datasets, 39 HC vs 34 AD)					
GSE36980	19	10	GPL6244 [HuGene-1_0-st] Affymetrix Human Gene 1.0 ST Array [transcript (gene) version]	Japan	Yusaku Nakabeppu
GSE37263	8	8	GPL5175 [HuEx-1_0-st] Affymetrix Human Exon 1.0 ST Array [transcript (gene) version]	Singapore	Michelle GK Tan
GSE5281	12	16	GPL570 [HG-U133_Plus_2] Affymetrix Human Genome U133 Plus 2.0 Array	USA	Winnie Liang
WB (4 datasets, 251 HC vs 296 AD)					
GSE97760	10	9	GPL16699 Agilent-039494 SurePrint G3 Human GE v2 8x60K Microarray 039381 (Feature Number version)	USA	Haiyan Fu
GSE63060	104	145	GPL6947 Illumina HumanHT-12 V3.0 expression beadchip	UK	Jamie Timmons
GSE63061	134	139	GPL10558 Illumina HumanHT-12 V4.0 expression beadchip	UK	Jamie Timmons
GSE18309	3	3	GPL570 [HG-U133_Plus_2] Affymetrix Human Genome U133 Plus 2.0 Array	Taiwan	Kuang-Den Chen

HC: healthy controls; AD: Alzheimer's disease; HIP: hippocampus; TG: temporal gyrus; FG: frontal gyrus; WB: whole blood.

which covered the gene expression profiling of HIP tissues generated from 22 AD patients and 9 healthy controls [18,26]. Box plot analysis was used to depict the expression levels of DEGs in AD patients and health individuals in GSE1297 dataset, which was visually illustrated by median and interquartile range.

ROC curve analysis

In order to detect the diagnostic value of DEGs in AD, pROC package in R language for depicting receiver operating characteristic (ROC) curves was used in this study and area under the curve (AUC) of ROC curves was calculated to assess the performance of each DEG. When AUC value was greater than 0.6, the DEG was considered capable of distinguishing case and normal controls. The diagnostic value of DEGs in GSE63060 and GSE63061 datasets was assessed in our work.

Statistical analysis

The statistical significance of differences between groups was assessed using the unpaired Student's

t test. $p < .05$ was considered as a significant difference. * indicates $p < .05$; ** indicates $p < .01$ and *** indicates $p < .001$.

Results

DEGs in AD

The respective DEGs in HIP, FG and TG were respectively identified. As Figure 1 shows, DEGs could clearly discriminate AD from controls in HIP, FG and TG brain regions. Among the DEGs, 325 common DEGs (177 up-regulated and 148 down-regulated DEGs) were overlapped from HIP, FG and TG (Figure 2(A)).

Dysregulated biological processes in AD brain

We investigated the biological processes of DEGs in AD. As Figure S1A, S1B and S1C shows, functions related to apoptosis were significantly enriched in HIP, TG and FG, including regulation of apoptotic process, apoptotic process and cell death. Moreover, the biological processes of common DEGs overlapped from HIP, FG and TG were enriched. As Table 2 shows,

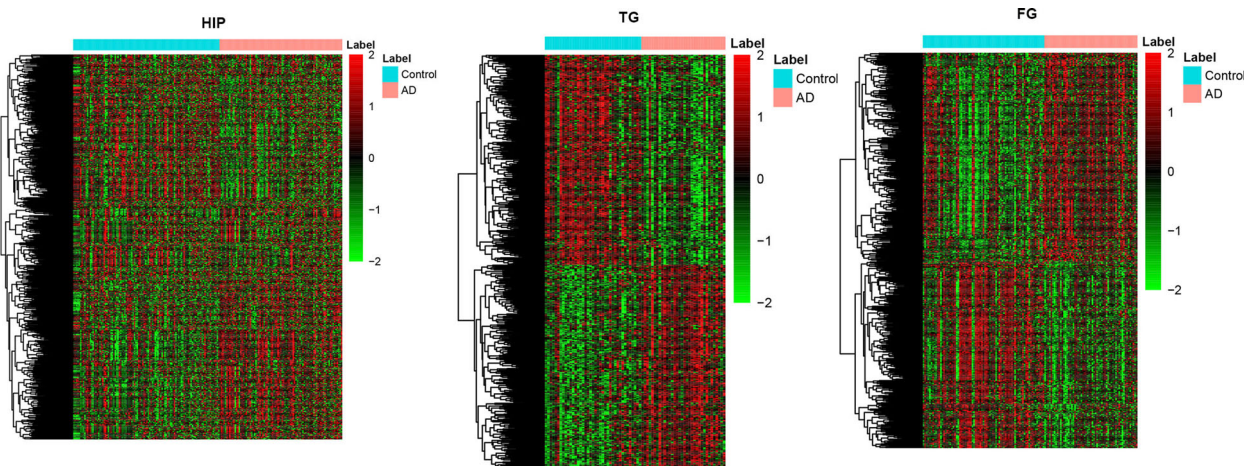


Figure 1. The heat maps of DEGs in AD patients and healthy individuals. A: the heat map of DEGs in HIP tissue; B: the heat map of DEGs in TG tissue; C: the heat map of DEGs in FG tissue.

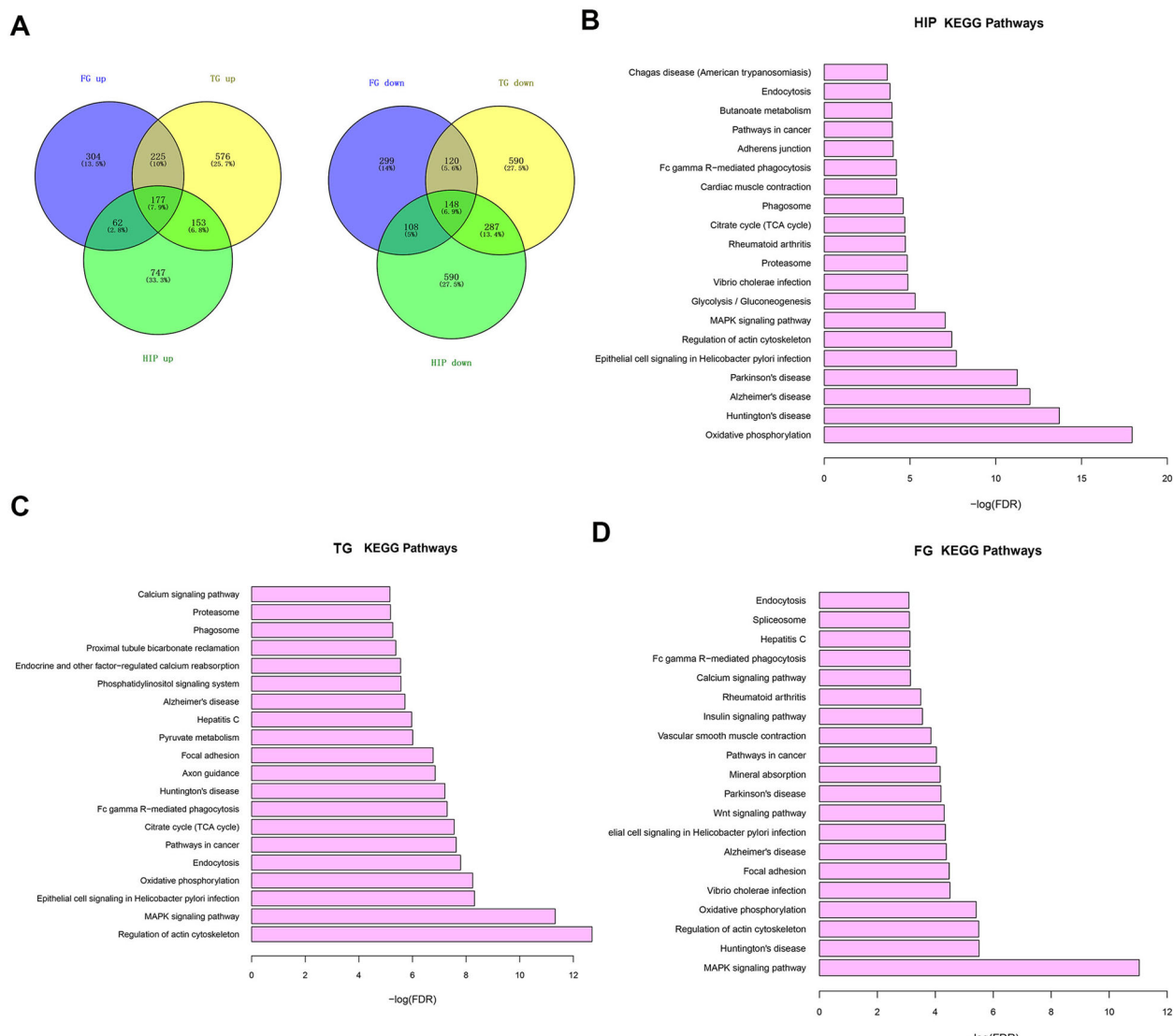


Figure 2. The enriched pathways of DEGs in HIP, TG and FG tissues of AD. A: the overlapped DEGs in HIP, TG and FG; B: the enriched pathway of DEGs in HIP tissue; C: the enriched pathway of DEGs in TG tissue; D: the enriched pathway of DEGs in FG tissues.

Table 2. Biological process and KEGG pathway of common DEGs in AD.

Items	Items_Details	FDR
Biological process		
GO:0008285	negative regulation of cell proliferation (BP)	7.3986E-05
GO:0006810	transport (BP)	0.00144644
GO:0007399	nervous system development (BP)	0.00308066
GO:0055085	transmembrane transport (BP)	0.00312548
GO:0007165	signal transduction (BP)	0.0032394
GO:0070371	ERK1 and ERK2 cascade (BP)	0.00336544
GO:0045892	negative regulation of transcription, DNA-dependent (BP)	0.00379911
GO:0008284	positive regulation of cell proliferation (BP)	0.00998021
GO:0001701	in utero embryonic development (BP)	0.0128138
GO:0030097	hemopoiesis (BP)	0.0143162
GO:0006112	energy reserve metabolic process (BP)	0.0163187
GO:0006921	cellular component disassembly involved in apoptosis (BP)	0.0289097
GO:0006915	apoptotic process (BP)	0.0304084
GO:0007275	multicellular organismal development (BP)	0.0306591
GO:0045893	positive regulation of transcription, ODNA-dependent (BP)	0.0323205
GO:0000122	negative regulation of transcription from RNA polymerase II promoter (BP)	0.0353817
GO:0042493	response to drug (BP)	0.037461
GO:0008283	cell proliferation (BP)	0.0453469
GO:0010628	positive regulation of gene expression (BP)	0.0480963
GO:0045944	positive regulation of transcription from RNA polymerase II promoter (BP)	0.0486373
KEGG pathway		
Kegg:04810	Regulation of actin cytoskeleton	0.00028761
Kegg:04010	MAPK signaling pathway	0.00014954

FDR: false discovery rate; BP: biological process; KEGG: Kyoto Encyclopedia of Genes and Genomes; GO: gene ontology; DEG: differentially expressed gene; AD: Alzheimer's disease.

negative regulation of cell proliferation, nervous system development, ERK1 and ERK2 cascade, and apoptotic process were significantly enriched.

Dysregulated biological pathways in AD brain

We also investigated the biological pathways of DEGs in AD. As Figure 2(B), 2(C) and 2(D) shows, DEGs related to the Alzheimer's disease, Huntington's disease and MAPK signaling pathway were significantly enriched in HIP, TG and FG. Pathway involved in adhesions junction was significantly enriched in HIP (Figure 2(B)). Wnt signaling pathway was significantly enriched in FG (Figure 2(D)). Moreover, the KEGG pathways of common DEGs overlapped from HIP, FG and TG were enriched. As Table 2 shows, regulation of actin cytoskeleton and MAPK signaling pathway was significantly enriched.

Protein–protein interaction network in AD brain

The protein–protein interaction (PPI) network of top 20 up- and down-regulated DEGs in HIP, TG and FG was respectively deciphered. In PPI network of HIP (Figure 3), YAP1 had the high connectivity with DEGs, which interacted with 18 DEGs. In PPI network of TG (Figure S2), MAPK9 had the high connectivity with DEGs, which interacted with 16 DEGs. In PPI network of FG (Figure S3), GJA1 had the high connectivity with DEGs, which interacted with six DEGs.

The common DEGs in whole blood and AD brain regions

A total of 2101 DEGs of WB samples of AD were identified. As Figure 4(A) shows, DEGs could clearly discriminate AD from controls. Forty common DEGs (22 up-regulated DEGs and 18 down-regulated DEGs) were overlapped from DEGs in HIP, TG, FG and WB (Figure 4(B)). Those DEGs were significantly enriched in adipocytokine signaling pathway, cytokine–cytokine receptor interaction and Alzheimer's disease (Figure 4(C)). As Figure 5 shows, in PPI network, TNFRSF1A and MAP3K5 had the high connectivity with DEGs, which respectively interacted with 152 and 76 DEGs.

The expression levels of common DEGs were analyzed in GSE1297 dataset

GSE1297 covered the expression profiling of HIP tissues from 22 AD patients and 9 health individuals. In our work, 35 out of 40 common DEGs were identified in GSE1297 dataset. The mRNA expression levels of 31 common DEGs were consistent with our integrated analysis. The expression of 14 out of 31 common DEGs was significantly changed. As Figure 6(A–J) shows, ARHGEF40, WWC3, VCAN, SSH3, SAFB2, LRCH4, IL10RA, CDK13, BBX and SPSB3 were significantly up-regulated in HIP; in addition, MRPL15, COPS3, TXNDC9 and RAD51C were significantly down-regulated in HIP compared to HC (Figure 6(K–N)).

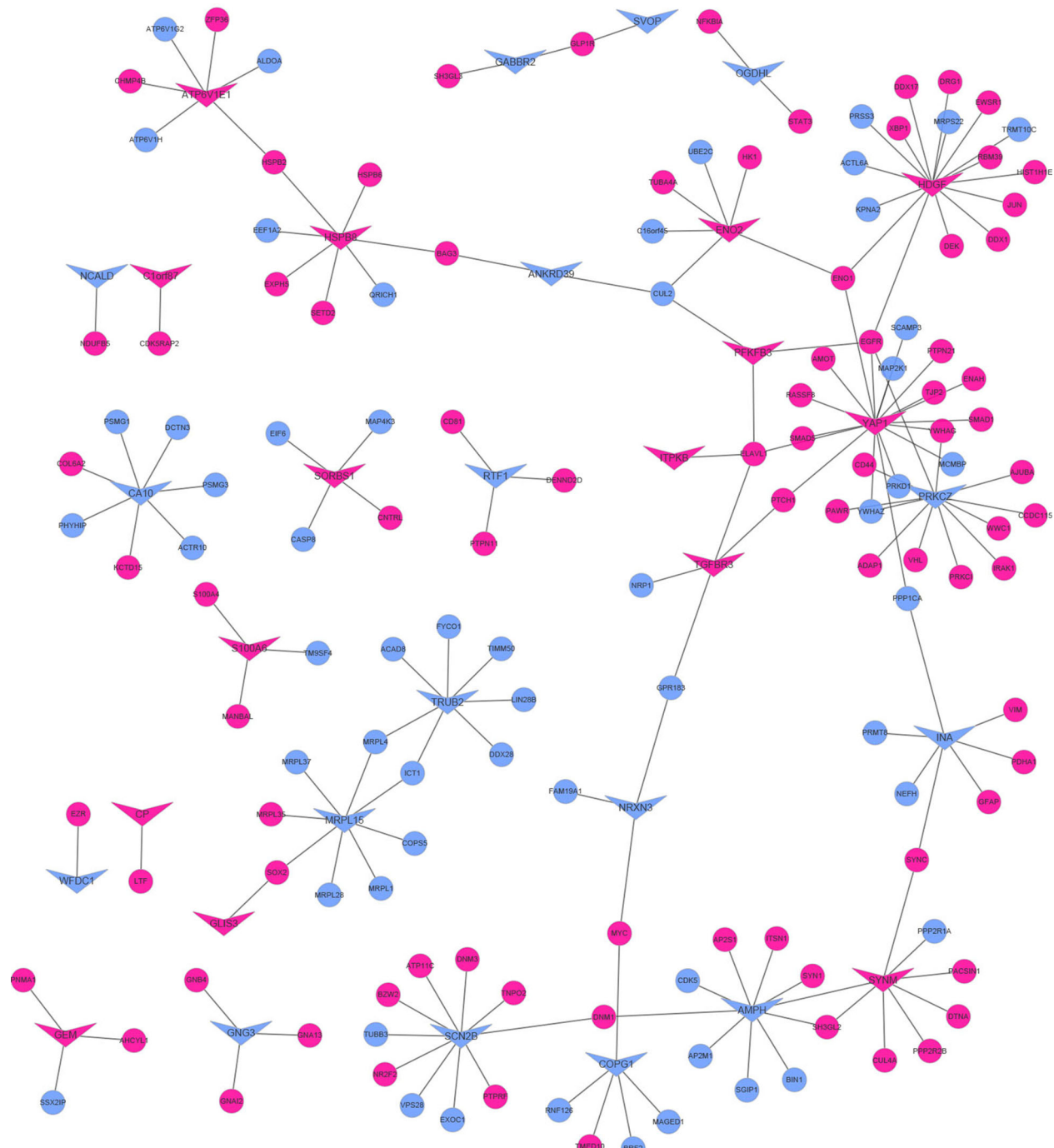


Figure 3. The protein–protein interaction network of top 20 up- and down-regulated DEGs in HIP tissues of AD. Rose and blue triangle nodes indicated top 20 up- and down-regulated DEGs in HIP, respectively. Rose and blue round nodes indicated up- and down-regulated DEGs in HIP, respectively.

ROC curve analysis

In order to detect the discriminatory ability of 14 common DEGs abovementioned among WB samples of AD patients and healthy individuals, the ROC analyses in GSE63060 and GSE63061 datasets were performed. In GSE63060, 13 out 14 DEGs could distinguish WB samples of AD patients from healthy controls. Moreover, 8

out 14 DEGs had the diagnostic value in distinguishing WB samples of AD patients from healthy controls in GSE630061. As Figures 7 and 8 show, seven DEGs including MRPL15, RAD51C, SAFB2, SSH3, TXNDC9, VCAN and WWC3 had the diagnostic value in distinguishing WB samples of AD patients from healthy controls in both GSE630060 and GSE630061 datasets.

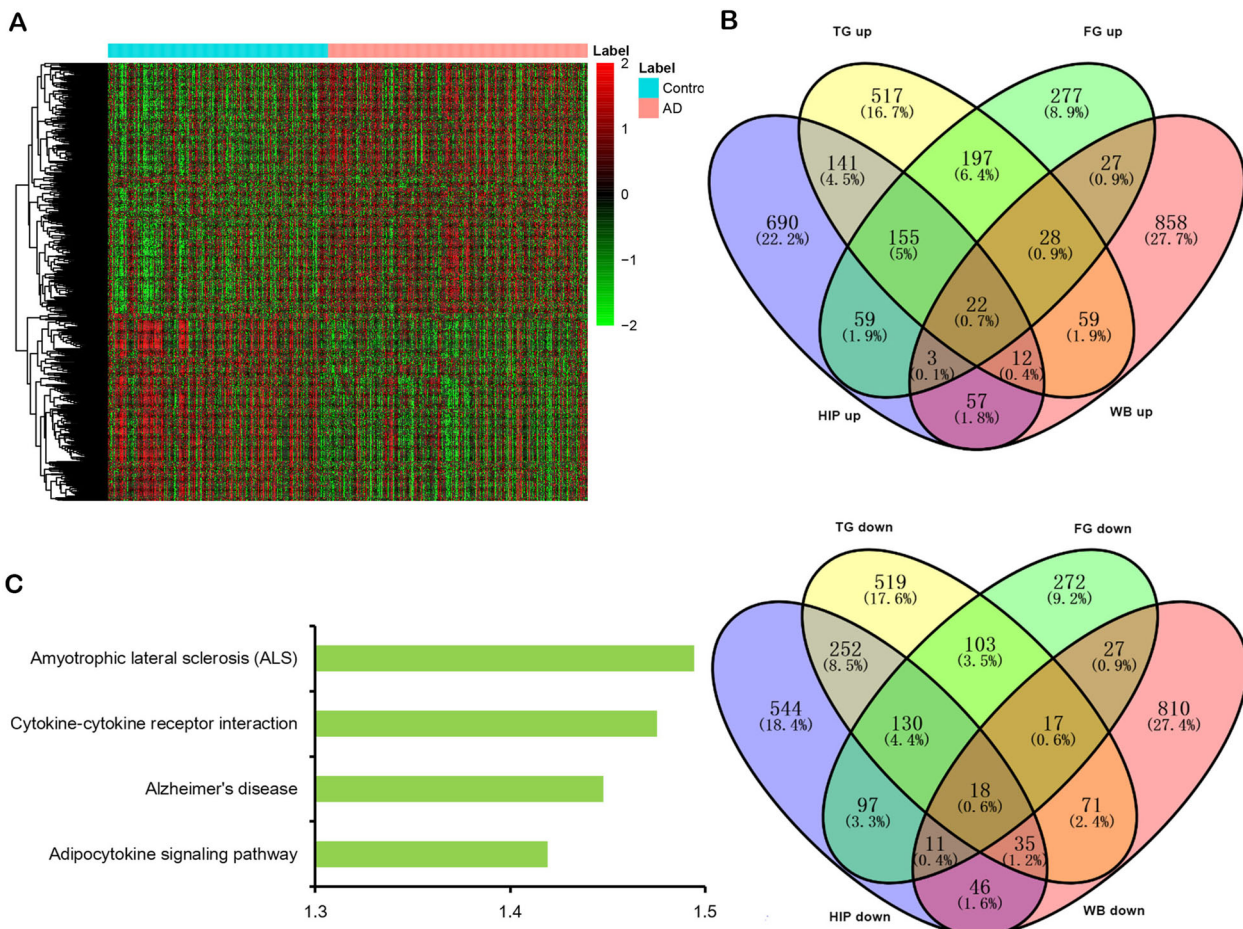


Figure 4. The common DEGs among HIP, TG, FG and whole blood in AD. A: the heatmap of DEGs in whole blood of AD; B: the common DEGs overlapped from HIP, TG, FG and whole blood; C: the enriched pathways of common DEGs in AD.

Discussion

Cell death mechanism is commonly found in AD. In our work, pathways related to apoptosis were significantly enriched in HIP, TG and FG, including regulation of apoptotic process, apoptotic process and cell death. It indicated that our bioinformatics analysis was acceptable.

TNFRSF1A, YAP1, MAPK1 and GJA1 were identified as key DEGs in AD in our work, and those genes involved in AD progression are documented. TNFRSF1A was significantly up-regulated and was enriched in MAPK signaling pathway and Alzheimer's disease in HIP, TG and FG. It is reported that binding of membrane-bound tumor necrosis factor-alpha (TNF-alpha) to the membrane-bound TNFRSF1A induces TNFRSF1A trimerization and activation, which plays a role in cell survival, apoptosis and inflammation [27]. Shang et al. [28] identify that TNFRSF1A associates with AD susceptibility in Caribbean Hispanic individuals through genome-wide haplotype association study. Steeland et al. demonstrate that TNFR1 contributes to the AD pathogenesis by mediating neuronal cell

death. In APP/PS1 transgenic mice, TNFR1 deficiency ameliorated amyloidosis [29].

In PPI network, YAP1, MAPK9 and GJA1 had the high connectivity with DEGs in HIP, TG and FG, respectively. Moreover, YAP1 and GJA1 were significantly up-regulated; MAPK9 was significantly down-regulated in HIP, TG and FG. YAP1 is a downstream nuclear effector of the Hippo signaling pathway, which is involved in development, growth, repair and homeostasis. Xu et al. demonstrate that knockdown of YAP1 expression leads to increased A β production and tau phosphorylation in U251-APP cells, whereas over-expression of YAP1 had opposite effects [30]. GJA1 is a component of gap junctions. Kajiwara et al. report that GJA1 is strongly associated with AD amyloid and tau pathologies. Astrocytes lacking *Gja1* show reduced Apoe protein levels as well as impaired A β phagocytosis. Wild-type neurons co-cultured with *Gja1*-/- astrocytes contain higher levels of A β species than those with wild-type astrocytes [31]. MAPK9 (also named as JNK2) and MAPK8 (also named as JNK1) belong to MAP kinase family. MAPK8 is significantly

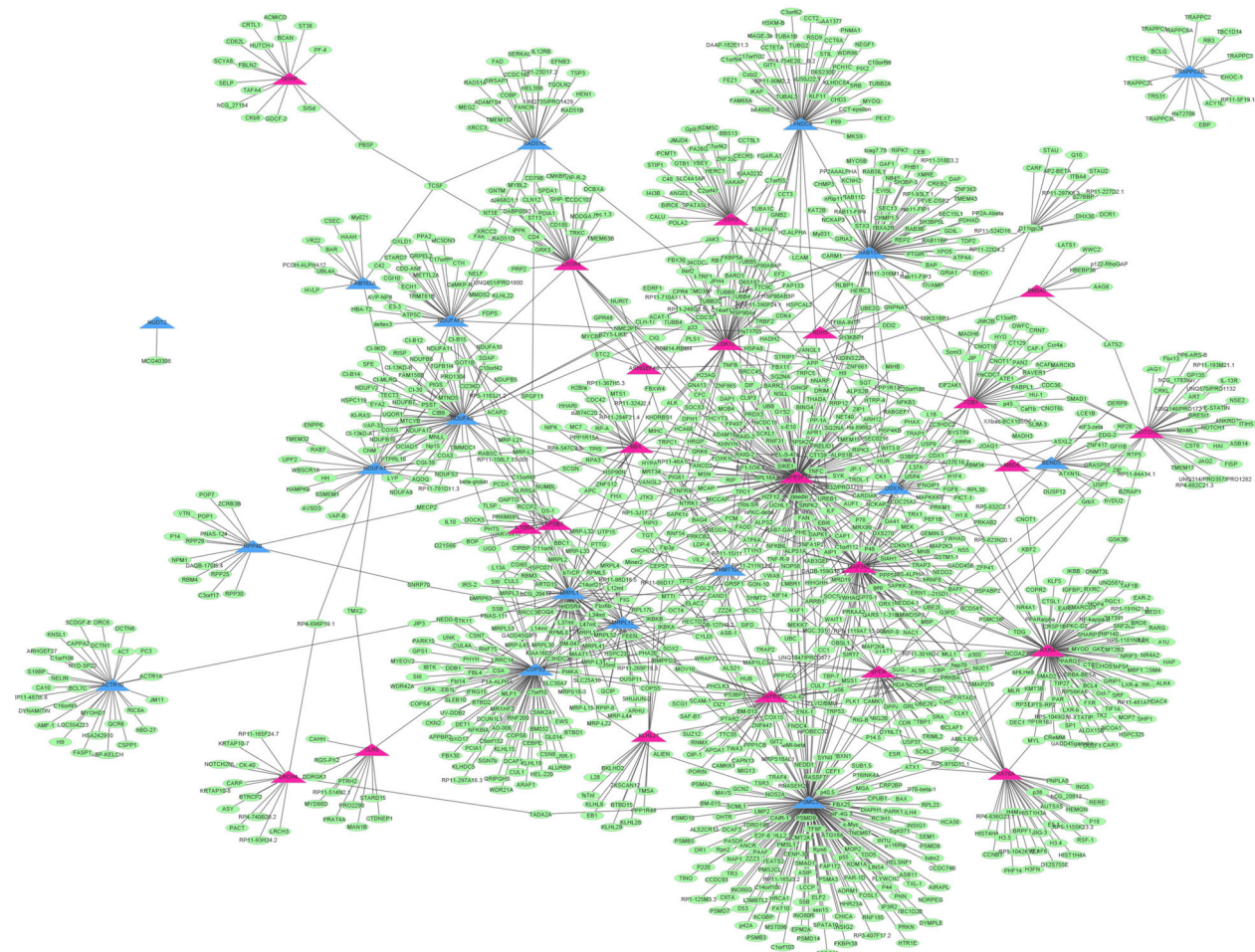


Figure 5. The protein–protein interaction network of common DEGs in AD. Rose and blue triangle nodes indicated up- and down-regulated common DEGs, respectively. Green node indicated DEGs in AD.

down-regulated in both HIP and TG. It is reported that JNKs are activated in degenerating neurons in AD [32]. Nicotinamide treatment significantly decreases β -amyloid production, amyloid plaque burden, synaptic loss and inflammatory responses in AD transgenic animals by the inhibition of JNK activation [33]. Wnt signaling pathway and MAPK signaling pathway were significantly enriched in AD. The canonical and non-canonical Wnt signaling pathways play neuroprotective roles in AD through modulation of mitochondrial processes [34]. Tapia-Rojas et al. report that Wnt signaling inhibitors induced severe changes in the hippocampus, including severe cognitive deficits, increased tau phosphorylation and A β 1-42 peptide levels, decreased A β 42/A β 40 ratio and A β 1-42 concentration in the cerebral spinal fluid, and high levels of soluble A β species and synaptotoxic oligomers in the hippocampus of AD mouse model [35,36]. Bhaskar's group report that p38 α MAPK inhibitor (MW108) suppresses p38 α MAPK activation, leading to reduced tau phosphorylation and preventing cognitive impairment in aged hTau mice [37,38].

Moreover, miR-330 plays a protective role in reducing amyloid β -protein production, alleviating oxidative stress and mitochondrial dysfunction in AD by targeting VAV1 via the MAPK signaling pathway [39].

Up to now, the clinical value of GJA1, YAP1 and MAPK9 in AD diagnosis has not been documented. The clinical value of hub genes in discriminating AD from healthy controls in early diagnosis would be explored in our further work.

MRPL15, RAD51C, SAFB2, SSH3, TXNDC9, VCAN and WWC3 could distinguish WB samples of AD patients from healthy individuals. The biological functions of those seven DEGs in AD have not been documented. However, the present studies demonstrate that those DEGs are involved in other diseases including cancers. Sotgiol et al. report that four mitochondrial proteins (MRPL15, HSPD1, UQCRCB and COX17), as a diagnostic signature, successfully predict distant metastasis in breast cancer [40]. It is reported that RAD51C is a cancer susceptibility gene and is linked to breast cancer, ovarian cancer and gastric cancer [41–43].

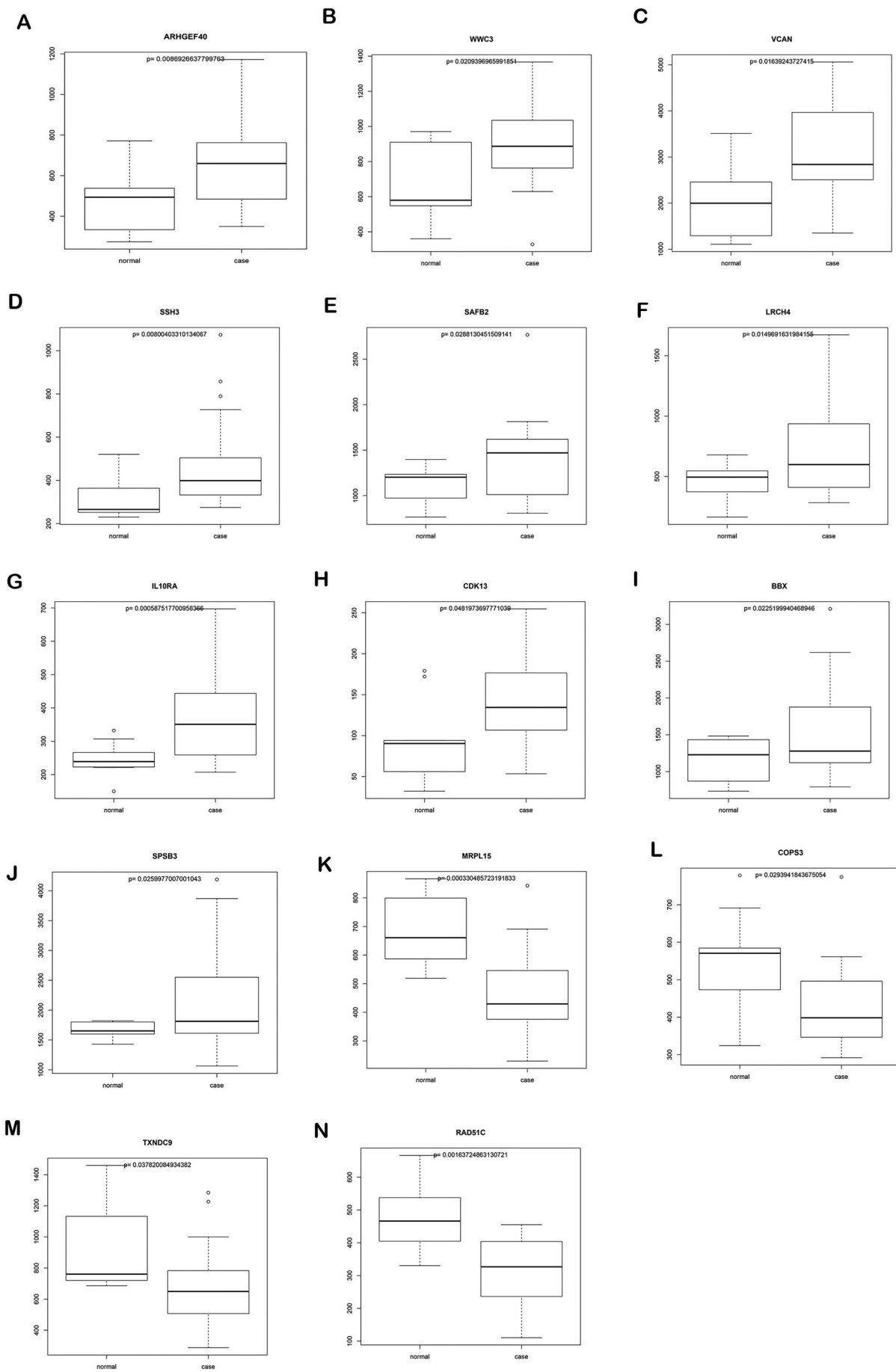


Figure 6. The expression level of common DEGs was analyzed in the GSE1297 dataset. Box plot diagram was used to describe the median and inter-quartile range of DEGs expression including (A), ARHGEF49 (B), WWC3 (C), VCAN (D), SSH3 (E), SAFB2 (F), LRCH4 (G), IL10RA (H), CDK13 (I), BBX, (J) SPSB3, (K), MRPL15 (L), COPS3 (M), TXNDC3 (N), RAD51C.

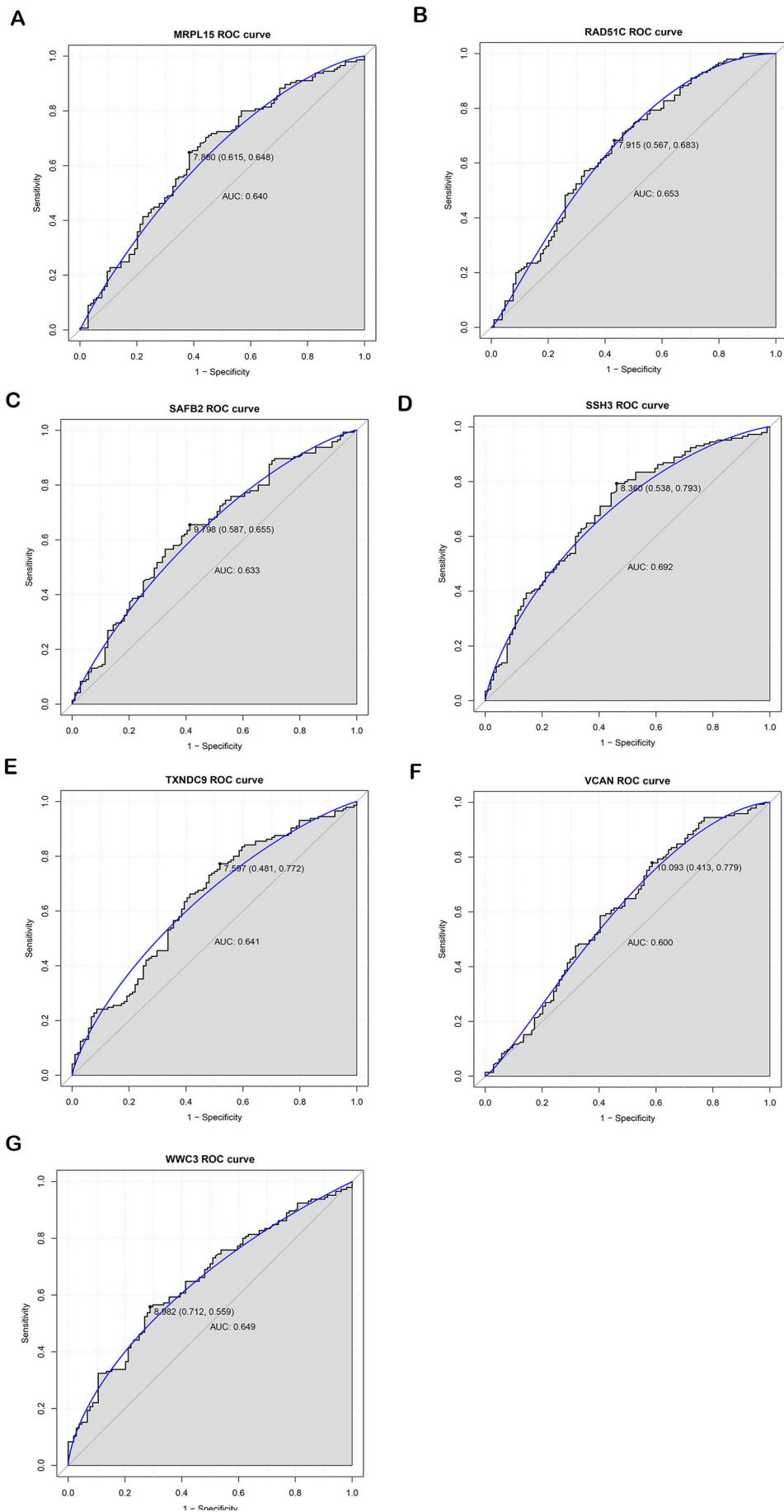


Figure 7. The discriminatory ability of common DEGs between AD patients and healthy controls was analyzed using an ROC curve in GSE63060 dataset. (A), MRPL15 (B), RAD51C; (C), SAFB2 (D), SSH3 (E), TXNDC9 (F), VCAN (G), WWC3.

Overexpression of RAD51C is associated with resistance to cisplatin and radiation in non-small cell lung cancer and predicts poor prognostic outcome [44]. Scaffold attachment factor B1 (SAFB1) and SAFB2, two homologous proteins, show high similarity, and functional domains are highly conserved [45]. SAFB1 interacts with and suppresses the transcriptional activity of p53, the gene that tightly associates with cell apoptosis, senescence and DNA repair [46]. SAFB1 mediates repression apoptotic genes including BBC3, NEDD9 and OPG in breast cancer cells [47]. The expression of TXNDC9 is correlated with tumor invasion, tumor size and TXNDC9-negative patients having shorter life spans in colorectal cancer [48]. Overexpression of WWC3 inhibits the glioma cell proliferation through suppressing the Wnt/β-catenin signaling pathway [49].

There are limitations in our study. Firstly, seven DEGs with the diagnostic value in distinguishing WB samples of AD patients from healthy individuals were identified. However, the diagnostic value of seven DEGs in large cohort of AD patients and healthy controls in clinical was not stated. Secondly, the biological functions of seven DEGs were not elaborated in AD progression in our work. In summary, the DEGs in three brain regions including HIP, TG and FG of AD patients were identified; the biological functions of DEGs were predicted through pathway enrichment and the construction of PPI network. The expression levels of 40 common DEGs in HIP, TG, FG and WB were primarily validated in GSE1297 dataset covering mRNA expression profiling of HIP tissues. The diagnostic value of common DEGs in distinguishing WB samples of AD patients from healthy controls in GSE630060 and GSE630061 datasets was detected.

Conclusion

Our work indicated that DEGs including TNFRSF1A, YAP1, MAPK1 and GJA1 might play key roles in pathogenesis in AD. Seven DEGs including MRPL15, RAD51C, SAFB2, SSH3, TXNDC9, VCAN and WWC3 might be potential diagnostic biomarkers in AD.

Disclosure statement

No potential conflict of interest was reported by the author(s).

References

- [1] Querfurth HW, LaFerla FM. Alzheimer's disease. *N Engl J Med.* 2010;362(4):329–344. [published Online First: 2010/01/29]
- [2] Serrano-Pozo A, Frosch MP, Masliah E, et al. Neuropathological alterations in Alzheimer disease. *Cold Spring Harbor Perspect Med.* 2011;1(1): a006189–a006189. [published Online First: 2012/01/10]
- [3] Liu SL, Wang C, Jiang T, et al. The role of Cdk5 in Alzheimer's disease. *Mol Neurobiol.* 2016;53(7): 4328–4342.
- [4] Gordon-Weeks PR. The role of the drebrin/EB3/Cdk5 pathway in dendritic spine plasticity, implications for Alzheimer's disease. *Brain Res Bull.* 2016;126(Pt 3): 293–299.
- [5] Wu Y, Ly PT, Song W. Aberrant expression of RCAN1 in Alzheimer's pathogenesis: a new molecular mechanism and a novel drug target. *Mol Neurobiol.* 2014; 50(3):1085–1097.
- [6] Gao L, Jiang T, Yao X, et al. TREM2 and the progression of Alzheimer's disease. *CNR.* 2017;14(2):177–183.
- [7] Jay TR, Hirsch AM, Broihier ML, et al. Disease progression-dependent effects of TREM2 deficiency in a mouse model of Alzheimer's disease. *J Neurosci.* 2017;37(3):637–647.
- [8] Perez SE, Nadeem M, He B, et al. Neocortical and hippocampal TREM2 protein levels during the progression of Alzheimer's disease. *Neurobiol Aging.* 2017;54: 133–143.
- [9] Uddin MS, Mamun AA, Labu ZK, et al. Autophagic dysfunction in Alzheimer's disease: cellular and molecular mechanistic approaches to halt Alzheimer's pathogenesis. *J Cell Physiol.* 2019;234(6):8094–8112. [published Online First: 2018/10/27]
- [10] Hossain MF, Uddin MS, Uddin GMS, et al. Melatonin in Alzheimer's disease: a latent endogenous regulator of neurogenesis to mitigate Alzheimer's neuropathology. *Mol Neurobiol.* 2019;56(12):8255–8276. [published Online First: 2019/06/19]
- [11] Uddin MS, Kabir MT. Emerging signal regulating potential of genistein against Alzheimer's disease: a promising molecule of interest. *Front Cell Dev Biol.* 2019;7:197. [published Online First: 2019/10/18]
- [12] Barrett T, Wilhite SE, Ledoux P, et al. NCBI GEO: archive for functional genomics data sets—update. *Nucleic Acids Res.* 2012;41(D1):D991–5. [published Online First: 2012/11/30]
- [13] Blair LJ, Nordhues BA, Hill SE, et al. Accelerated neurodegeneration through chaperone-mediated oligomerization of tau. *J Clin Invest.* 2013;123(10): 4158–4169. [published Online First: 2013/09/04]
- [14] Miller JA, Woltjer RL, Goodenbour JM, et al. Genes and pathways underlying regional and cell type changes in Alzheimer's disease. *Genome Med.* 2013; 5(5):48. [published Online First: 2013/05/28]
- [15] Hokama M, Oka S, Leon J, et al. Altered expression of diabetes-related genes in Alzheimer's disease brains: the Hisayama study. *Cerebral cortex (New York, NY: 1991).* 2014;24(9):2476–2488. [published Online First: 2013/04/19]
- [16] Blalock EM, Buechel HM, Popovic J, et al. Microarray analyses of laser-captured hippocampus reveal distinct gray and white matter signatures associated with incipient Alzheimer's disease. *J Chem Neuroanat.*

- 2011;42(2):118–126. [published Online First: 2011/07/16]
- [17] Readhead B, Haure-Mirande JV, Funk CC, et al. Multiscale analysis of independent Alzheimer's cohorts finds disruption of molecular, genetic, and clinical networks by human herpesvirus. *Neuron*. 2018;99(1):64–82 e7. [published Online First: 2018/06/26]
- [18] Blalock EM, Geddes JW, Chen KC, et al. Incipient Alzheimer's disease: microarray correlation analyses reveal major transcriptional and tumor suppressor responses. *PNAS*. 2004;101(7):2173–2178. [published Online First: 2004/02/11]
- [19] Tan MG, Chua WT, Esiri MM, et al. Genome wide profiling of altered gene expression in the neocortex of Alzheimer's disease. *J Neurosci Res*. 2010;88(6):1157–1169. [published Online First: 2009/11/26]
- [20] Naughton BJ, Duncan FJ, Murrey DA, et al. Blood genome-wide transcriptional profiles reflect broad molecular impairments and strong blood-brain links in Alzheimer's disease. *JAD*. 2014;43(1):93–108. [published Online First: 2014/08/01]
- [21] Sood S, Gallagher IJ, Lunnon K, et al. A novel multi-tissue RNA diagnostic of healthy ageing relates to cognitive health status. *Genome Biol*. 2015;16(1):185. [published Online First: 2015/09/08]
- [22] Marot G, Foulley JL, Mayer CD, et al. Moderated effect size and P-value combinations for microarray meta-analyses. *Bioinformatics* (Oxford, England). 2009;25(20):2692–2699. [published Online First: 2009/07/25]
- [23] Tabas-Madrid D, Nogales-Cadenas R, Pascual-Montano A. GeneCodis3: a non-redundant and modular enrichment analysis tool for functional genomics. *Nucleic Acids Res*. 2012;40(W1):W478–83. [published Online First: 2012/05/11]
- [24] Chatr-Aryamontri A, Oughtred R, Boucher L, et al. The BioGRID interaction database: 2017 update. *Nucleic Acids Res*. 2017;45(D1):D369–D79. [published Online First: 2016/12/17]
- [25] Shannon P, Markiel A, Ozier O, et al. Cytoscape: a software environment for integrated models of biomolecular interaction networks. *Genome Res*. 2003;13(11):2498–2504. [published Online First: 2003/11/05]
- [26] Lee HM, Sugino H, Aoki C, et al. Underexpression of mitochondrial-DNA encoded ATP synthesis-related genes and DNA repair genes in systemic lupus erythematosus. *Arthritis Res Ther*. 2011;13(2):R63. [published Online First: 2011/04/19]
- [27] Grabinger T, Bode KJ, Demgenski J, et al. Inhibitor of apoptosis protein-1 regulates tumor necrosis factor-mediated destruction of intestinal epithelial cells. *Gastroenterology*. 2017;152(4):867–879. [published Online First: 2016/11/28]
- [28] Shang Z, Lv H, Zhang M, et al. Genome-wide haplotype association study identify TNFRSF1A, CASP7, LRP1B, CDH1 and TG genes associated with Alzheimer's disease in Caribbean Hispanic individuals. *Oncotarget*. 2015;6(40):42504–42514. [published Online First: 2015/12/02]
- [29] Steeland S, Gorle N, Vandendriessche C, et al. Counteracting the effects of TNF receptor-1 has therapeutic potential in Alzheimer's disease. *EMBO Mol Med*. 2018;10(4):e8300. [published Online First: 2018/02/24]
- [30] Xu M, Zhang DF, Luo R, et al. A systematic integrated analysis of brain expression profiles reveals YAP1 and other prioritized hub genes as important upstream regulators in Alzheimer's disease. *Alzheimer's & Dementia*. 2018;14(2):215–229. [published Online First: 2017/09/20]
- [31] Kajiwara Y, Wang E, Wang M, et al. GJA1 (connexin43) is a key regulator of Alzheimer's disease pathogenesis. *Acta Neuropathol Commun*. 2018;6(1):144. [published Online First: 2018/12/24]
- [32] Zhu X, Raina AK, Rottkamp CA, et al. Activation and redistribution of c-jun N-terminal kinase/stress activated protein kinase in degenerating neurons in Alzheimer's disease. *J Neurochem*. 2001;76(2):435–441.
- [33] Yao Z, Yang W, Gao Z, et al. Nicotinamide mononucleotide inhibits JNK activation to reverse Alzheimer disease. *Neurosci Lett*. 2017;647:133–140.
- [34] Arrazola MS, Silva-Alvarez C, Inestrosa NC. How the Wnt signaling pathway protects from neurodegeneration: the mitochondrial scenario. *Front Cell Neurosci*. 2015;9:166. [published Online First: 2015/05/23]
- [35] Tapia-Rojas C, Inestrosa NC. Wnt signaling loss accelerates the appearance of neuropathological hallmarks of Alzheimer's disease in J20-APP transgenic and wild-type mice. *J Neurochem*. 2018;144(4):443–465. [published Online First: 2017/12/15]
- [36] Tapia-Rojas C, Inestrosa NC. Loss of canonical Wnt signaling is involved in the pathogenesis of Alzheimer's disease. *Neural Regen Res*. 2018;13(10):1705–1710. [published Online First: 2018/08/24]
- [37] Watterson DM, Grum-Tokars VL, Roy SM, et al. Development of novel *in vivo* chemical probes to address CNS protein kinase involvement in synaptic dysfunction. *PloS One*. 2013;8(6):e66226. [published Online First: 2013/07/11]
- [38] Lee JK, Kim NJ. Recent advances in the inhibition of p38 MAPK as a potential strategy for the treatment of Alzheimer's disease. *Molecules (Basel, Switzerland)*. 2017;22(8):1287. [published Online First: 2017/08/03]
- [39] Zhou Y, Wang ZF, Li W, et al. Protective effects of microRNA-330 on amyloid beta-protein production, oxidative stress, and mitochondrial dysfunction in Alzheimer's disease by targeting VAV1 via the MAPK signaling pathway. *J Cell Biochem*. 2018;119(7):5437–5448. [published Online First: 2018/01/26]
- [40] Sotgia F, Fiorillo M, Lisanti MP. Mitochondrial markers predict recurrence, metastasis and tamoxifen-resistance in breast cancer patients: early detection of treatment failure with companion diagnostics. *Oncotarget*. 2017;8(40):68730–68745.
- [41] Sanchez-Bermudez AI, Sarabia-Meseguer MD, Garcia-Aliaga A, et al. Mutational analysis of RAD51C and RAD51D genes in hereditary breast and ovarian cancer families from Murcia (southeastern Spain). *Eur J Med Genet*. 2018;61(6):355–361. [published Online First: 2018/02/08]
- [42] Sato K, Koyasu M, Nomura S, et al. Mutation status of RAD51C, PALB2 and BRIP1 in 100 Japanese familial breast cancer cases without BRCA1 and BRCA2

- [43] mutations. *Cancer Sci.* 2017;108(11):2287–2294. [published Online First: 2017/08/11]
- [44] Sahasrabudhe R, Lott P, Bohorquez M, et al. Germline mutations in PALB2, BRCA1, and RAD51C, which regulate DNA recombination repair, in patients with gastric cancer. *Gastroenterology.* 2017;152(5):983–986 e6. [published Online First: 2016/12/28]
- [45] Chen X, Qian D, Cheng J, et al. High expression of Rad51c predicts poor prognostic outcome and induces cell resistance to cisplatin and radiation in non-small cell lung cancer. *Tumor Biol.* 2016;37(10):13489–13498. [published Online First: 2016/07/29]
- [46] Oesterreich S. Scaffold attachment factors SAFB1 and SAFB2: innocent bystanders or critical players in breast tumorigenesis? *J Cell Biochem.* 2003;90(4):653–661. [published Online First: 2003/10/31]
- [47] Peidis P, Voukkalis N, Aggelidou E, et al. SAFB1 interacts with and suppresses the transcriptional activity of p53. *FEBS Lett.* 2011;585(1):78–84.
- [48] Hammerich-Hille S, Kaipparettu BA, Tsimelzon A, et al. SAFB1 mediates repression of immune regulators and apoptotic genes in breast cancer cells. *J Biol Chem.* 2010;285(6):3608–3616.
- [49] Lu A, Wangpu X, Han D, et al. TXNDC9 expression in colorectal cancer cells and its influence on colorectal cancer prognosis. *Cancer Invest.* 2012;30(10):721–726. [published Online First: 2012/12/06]
- [50] Wang Y, Jiang M, Yao Y, et al. WWC3 inhibits glioma cell proliferation through suppressing the Wnt/beta-catenin signaling pathway. *DNA Cell Biol.* 2018;37(1):31–37. [published Online First: 2017/11/09]